International Journal of Mechanical Engineering

Mathematical Modeling and Analysis of Composite Fully Elliptic Spring Elements

Subramanian Muthusamy
Department of Automobile Engineering, PSG College of Technology, Coimbatore 641004, India.
muthusamy.subramanian@gmail.com

Niresh. J
Department of Automobile Engineering, PSG College of Technology, Coimbatore 641004, India.

Neelakrishnan Subramaniyan
Department of Automobile Engineering, PSG College of Technology, Coimbatore 641004, India.
[1]msn.auto@psgtech.ac.in;

Abstract:

In this paper E-glass/epoxy fully elliptic spring elements were analytically modeled based on classical laminate theory (CLT) and strain energy methods. The mid-plane symmetric laminated spring element has amajor axis/minor axis ratio (a/b ratio) of 1.5. The mechanical properties such as spring rate, point of contraflexure, stress and strain distributions under uniaxial loading have been computed and analyzed.The effect of variables such as a/b ratio, width, thickness, volume fraction of fibres (V_f) and laminate configuration on the spring stiffness have been studied. In the experimental part spring elements of various configurations were fabricated using filament winding technique. The spring elements were loaded along the minor axis using an Universal Testing Machine. It was found to exhibit linear stiffness in the desired range of deflection. A close matching between theoretical and experimental values was observed. Based on these studies, the geometric parameters and laminate configuration of the spring element were optimized.

KEYWORDS: FRP, composite, elliptic spring element, bending strain energy, Castiglianos theorem.

INTRODUCTION

Polymer Matrix composites find lot of application in various disciplines of engineering due to their light weight, inherent damping and superior fatigue properties. Composite products are very vital to the light weighting of automotive vehicles. Commonly used products are composite drive shaft, instrument cluster, bumpers, battery covers and body panels. In addition to these, composite suspension springs such as monocoque leaf springs and fully elliptic springs have started gaining importance. Leaf springs can be used for rigid axle suspension and fully elliptic springs can be used in place of steel helical coil springs for independent suspension. The spring elements studied in the current work are intended to replace the conventional front suspension steel helical coil springs of the light motor vehicles (LMV).The proposed spring elements can be stacked over each other to form a complete spring. The major advantages of using the composite suspension springs are:
(ii). Superior vehicle ride characteristics owing to lower unsprung mass.
(iii) The higher inherent damping.
(iii) Superior fatigue characteristics.

So *et al (*1) have developed theoretical formulation for composite circular springelements bases bending strain energy (So *et al*, 1991). Castigliano's theorem was used to compute the spring deflection

Mahdi et al (2) have studied the influence of ellipticity ratio on performance of woven roving wrapped composite elliptical springs has been investigated both experimentally and numerically. This study demonstrated that composites semi-elliptical spring can be used for light and heavy trucks and meet the requirements, together with substantialweight saving. The results showed that the ellipticity ratio significantly influenced the spring rate and failure loads. Composite elliptic spring with ellipticity ratios of a/b 2.0 displayed the highest spring rate.

Abdul Rahim Abu Talib et al (3) have developed finite element models to optimize the material and geometry of the composite semi-elliptical spring based on the spring rate, log life and shear stress parameters. The influence of the ellipticity ratio on the performance of woven roving–

wrapped composite elliptical springs was investigated both experimentally and numerically.

Amol Bhanage and K. Padmanabhan (4) have evaluated the fatigue characteristics of GFRP leaf springs. It was found that the linear elastic stresses from Finite element analysis can be used directly to calculate fatigue damage. Also it is shown that, design and simulation stresses satisfying maximum stress failure criterion; hence design is safe

The authors Shivaji M. Mane and S B. Bhosale (5) have compared the experimental results of static performance of semi-elliptic spring elements with FEA analysis and found them to agree well.

Papacz et al (6) have studied the dynamic performance of steel and composite leaf elliptic springs. It is concluded that composite leaf springs have superior vibration absorption properties compared to steel spring.

P.K. Mallick (7) has investigated the Static Mechanical Performance of Fully elliptic Composite Springs elements. It was found that the primary failure mode in composite elliptic spring elements was interlaminar shear which occurred at or near the minor diameter. The spring elements are capable of absorbing large deformations, yet exhibit a linear behavior until the first interlaminar shear failure occurs. Both spring rate and maximum failure increase with increasing wall thickness

Tse et al (8) have formulated analytical expressions based on the principle of minimum potential energy are presented which describe the stiffnesses of mid-surface symmetric, woven composite circular springs with extended flat contact surfaces subject to unidirectional line and surface-loading configurations. Comparison studies of the results obtained from both the analytical and numerical models are made with experimental data, and the results are found to be satisfactory. The semi-included angle of the flat contact surface is vital parameter to spring stiffnesses of the composite spring..

Reid et al (9) have investigated the large deflection of composite circular springs with extended flat contact surfaces. Woven fibre/epoxy composite circular springs of range of different radii and thicknesses were fabricated and tested. FEA was used for theoretical analysis. Theoretical studies agree well with experimental results. The angular position of the zero-strain location increases linearly with the semi-included angle in the surface-loading configuration. However, it is always in the vicinity of 45 degree in the line-loading configuration

Tse et al (10) have developed analytical solution for circular composite spring element based on bending strain energy principles. The theoretical model was validated with experimental results.

NahitOztoprak et al (11) have studied the mono-composite leaf spring systems with different material configurations using three-dimensional FEM. The analysis results demonstrated that all the proposed designs experience stress levels below the yielding. Comparison of the predicted results with the experimental test results for the manufactured prototypes showed good agreement in terms of the load-displacement response

Zheng Yinhuan et al (12) have analysed the characteristics of a composite leaf spring made from glass fiber reinforced plastics using the ANSYS software. Considering interleaf contact, the stress distribution and deformation are obtained.

Anil Antony Sequeira et al (13) have carried out a Comparative Analysis of Helical Steel Springs with Composite Springs Using Finite Element Method' and found the results are closely matching. The load- deflection and stress – strain curves were plotted and found to be linear.

Mehdi Bakhshesh and Majid Bakhshesh (14) have replaced helical steel spring has by composite helical springs. Numerical results have been compared with experimental results and found to be in good agreement. Displacement in composite helical spring is more than that of steel spring and has the least value when fiber is oriented in the direction of loading.

Based on the above literature survey it is clear that glass fibre / epoxy matrix composite are most suitable for spring applications. The suspension system requirements are largely dependent on the type of vehicle. Generally, the spring stiffness varies from 20 N/mm to 40 N/mm.
This paper deals with the analytical formulation for the estimation of static mechanical properties of spring elements. The detailed theoretical formulation for composite elliptic spring elements has been presented.The results obtained from the theoretical analysis and the discussion are also presented.

Analytical Formulation of Composite Fully Elliptic Spring Elements

The typical isometric view of composite elliptic spring element is shown in Fig.1

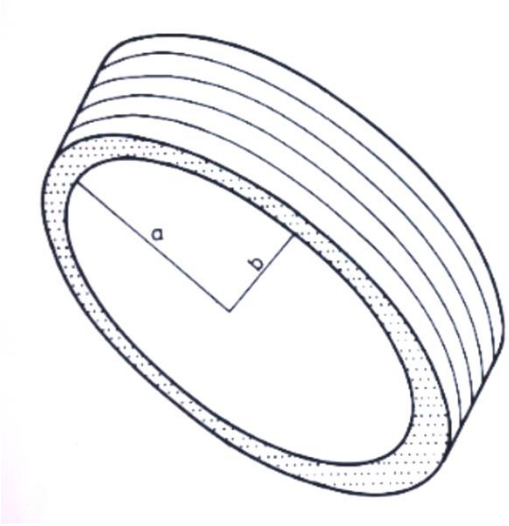

Fig. 1 Composite elliptic spring element

The theoretical formulation was carried out based on the following assumptions.

(i) Due to the bi-axial symmetry of the spring element, only one quadrant has been considered for the analysis.

(ii) The work done by the external loads on the spring element is absorbed in the form of bending strain energy. The effects of shear and axial strain energy are negligible.

The approach involves the following steps:

(i) The expression for bending strain energy (U_b) of one quadrant (0-90°) of the spring element has been derived.

(ii)Castigliano's first theorem was applied to calculate the spring deflection (□□ at the required point and the associated stiffness.

The notations used in the theoretical formulation are at the end of this manuscript

The methodology of analytical formulation is given in the following diagram

DR JN PLEASE CUT PASTE THE FLOW CHART HERE

The spring element is subjected to load (P) along its minor axis. The forces and moments acting on one quadrant of the spring element is given in Fig. 2. The mid-plane stress and moment resultants shown in Fig. 3

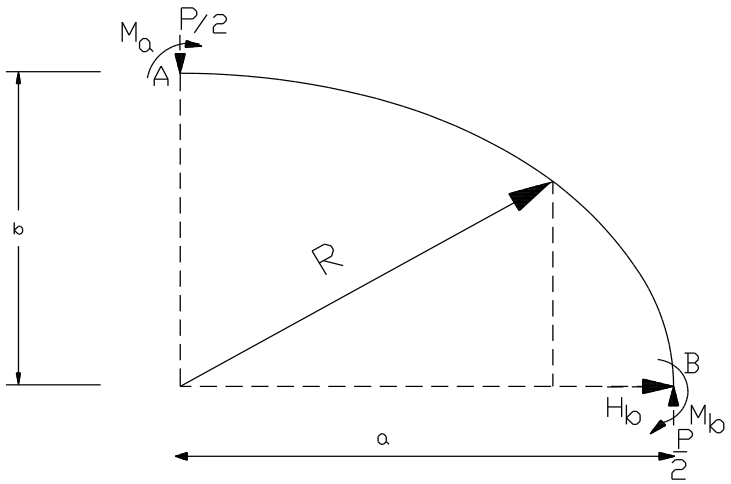

Fig 2Idealized one quadrant of the spring element showing the forces and moments

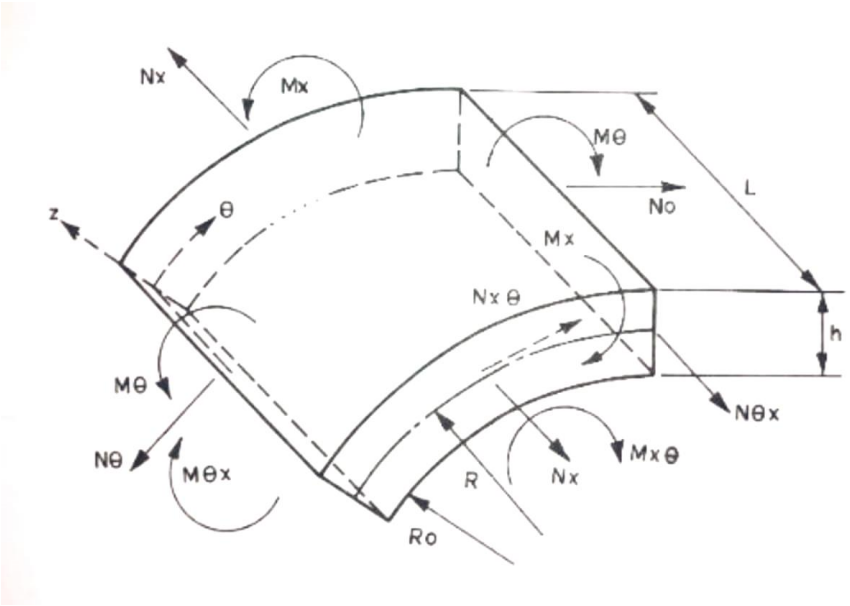

Fig. 3 The mid-plane stress and moment resultants

According to Classical Lamination Theory (CLT) for composite laminates the constitutive equation for an anisotropic laminate is given by

$$\begin{Bmatrix} N \\ M \end{Bmatrix} = \begin{bmatrix} A_{ij} & B_{ij} \\ B_{ij} & D_{ij} \end{bmatrix} \begin{Bmatrix} \varepsilon^{\circ} \\ \kappa \end{Bmatrix} \quad (1)$$

Elements of constitutive matrices are given as

$$A_{ij} = \sum_{k=1}^{n} Q_{ij} \left(h_k - h_{k-1}\right)$$

$$B_{ij} = \frac{1}{2} \sum_{k=1}^{n} Q_{ij} \left(h_k^2 - h_{k-1}^2\right)$$

$$D_{ij} = \frac{1}{3} \sum_{k=1}^{n} Q_{ij} \left(h_k^3 - h_{k-1}^3\right)$$

(h_k- h_{k-1}) = z (thickness of each layer)

$$\{N\} = [A] \left\{\varepsilon^{\circ}\right\} + [B] \{\kappa\}. \quad (2)$$

$$\{M\} = [B] \left\{\varepsilon^{\circ}\right\} + [D] \{\kappa\} \quad (3)$$

From equation 2

$$[A]^{-1}\{N\} = \left\{\varepsilon^{\circ}\right\} + [A]^{-1}[B] \{\kappa\}$$

or

$$\left\{ \varepsilon^{\circ} \right\} = [A]^{-1} \{N\} - [A]^{-1} [B] \{\kappa\} \quad (4)$$

Substituting equation 4 in equation 3

$$\{M\} = [B] \left[[A]^{-1} \{N\} - \left([A]^{-1} [B] \{\kappa\} \right) \right] + [D] \{\kappa\} \quad (5)$$

let

$$\left[A^*\right] = [A]^{-1}$$
$$\left[B^*\right] = -[A]^{-1}\ [B]$$
$$\left[C^*\right] = [B]\ [A]^{-1}$$
$$\left[D^*\right] = [D] - [B]\ [A]^{-1}\ [B] \quad (5a)$$

and equation 4 becomes

$$\left\{\varepsilon^\circ\right\} = \left[A^*\right]\ \{N\} + \left[B^*\right]\ \{\kappa\} \quad (6)$$

and equation 5 becomes

$$\{M\} = \left[C^*\right]\ \{N\} + \left[D^*\right]\ \{\kappa\}$$
$$\left[D^*\right]^{-1}\{M\} = \left[D^*\right]^{-1}\left[C^*\right]\ \{N\} + \ \{\kappa\}$$
$$\{\kappa\} = \left[D^*\right]^{-1}\{M\} - \left[D^*\right]^{-1}\left[C^*\right]\ \{N\} \quad (7)$$

Substituting equation 7 in equation 6

$$\left\{\varepsilon^\circ\right\} = \left[A^*\right]\ \{N\} + \left[B^*\right]\ \left[D^*\right]^{-1}\{M\} - \left[B^*\right]\left[D^*\right]^{-1}\left[C^*\right]\ \{N\}$$
$$\left\{\varepsilon^\circ\right\} = \left(\left[A^*\right] - \left[B^*\right]\left[D^*\right]^{-1}\left[C^*\right]\right)\{N\} + \left[B^*\right]\ \left[D^*\right]^{-1}\{M\} \quad (8)$$

let

$$\left[A'\right] = \left[A^*\right] - \left[B^*\right]\ \left[D^*\right]^{-1}\ \left[C^*\right]$$
$$\left[B'\right] = \left[B^*\right]\ \left[D^*\right]^{-1}$$
$$\left[C'\right] = -\left[D^*\right]^{-1}\ \left[C^*\right] \quad (9)$$
$$\left[D'\right] = \left[D^*\right]^{-1}$$

The equations 8 and 7 can be re-written as

$$\left\{\varepsilon^\circ\right\} = \left[A'\right]\ \{N\} + \left[B'\right]\ \{M\} \quad (10)$$

$$\{\kappa\} = \left[C'\right]\ \{N\} + \left[D'\right]\ \{M\} \quad (11)$$

From equations 10 and 11

$$\begin{Bmatrix} \varepsilon^\circ \\ \kappa \end{Bmatrix} = \begin{bmatrix} A' & B' \\ C' & D' \end{bmatrix} \begin{Bmatrix} N \\ M \end{Bmatrix} \quad (12)$$

Strain Energy Expression

The method of application of strain energy concepts to evaluate the stiffness of elliptic spring elements are given in the following. The elastic strain energy (U_b) is given by

$$U_b = \frac{1}{2}\int \sigma_{ij}\ \varepsilon_{ij}\ dv = \int_v W\, dv \quad (13)$$

The strain energy density function is

$$\left(\frac{dU_b}{dv}\right) = W = \frac{1}{2}\ \ \sigma_{ij}\varepsilon_{ij} \quad (14)$$

Assuming in-plane stress acting on the laminate, the strain at the k^{th} lamina can be given as

$$\{\varepsilon\}_k = \{\varepsilon^o\} + z\,\{\kappa\} \tag{15}$$

The stress at the kth lamina is given by

$$\{\sigma\}_k = [Q_k]\left[\{\varepsilon^\circ\} + z\,\{\kappa\}\right] \tag{16}$$

Now the strain energy function 'W' becomes

$$W = \tfrac{1}{2}\left[\{\varepsilon^\circ\} + z\,\{\kappa\}\right]^T [Q_k]\left[\{\varepsilon^\circ\} + z\,\{\kappa\}\right] \tag{17}$$

The strain energy density function for a cross-sectional area having width 'L' of a shell is given in the following.

$$W' = \sum_{k=1}^{n} \int_{h_{k-1}}^{h_k} W\,L\,dz = \sum_{k=1}^{n} \frac{1}{2} \int_{h_{k-1}}^{h_k} \sigma_{ij}\ \varepsilon_{ij}\ L\,dz \tag{18}$$

$$W' = \sum_{k=1}^{n} \int_{h_{k-1}}^{h_k} \frac{1}{2}\left(\{\varepsilon^\circ\} + z\,\{\kappa\}\right)^T [Q]_k \left(\{\varepsilon^\circ\} + z\,\{\kappa\}\right) L\,dz \tag{19}$$

All the matrices are independent of 'z'. On integrating and substituting the limits, W' can be written as given in the following.

$$W' = \sum_{k=1}^{n} \frac{L}{2} \begin{Bmatrix} \left(h_k - h_{k-1}\right)\{\varepsilon^\circ\}^T [Q]_k \{\varepsilon^\circ\} + \frac{1}{2}\left(h_k^2 - h_{k-1}^2\right)\{\varepsilon^\circ\}^T [Q]_k \{\kappa\} + \\ \frac{1}{2}\left(h_k^2 - h_{k-1}^2\right)\{\kappa\}^T [Q]_k \{\varepsilon^\circ\} + \frac{1}{3}\left(h_k^3 - h_{k-1}^3\right)\{\kappa\}^T [Q]_k \{\kappa\} \end{Bmatrix} \tag{20}$$

It is well known that

$$[N] = Q_{ij}\left\{\left(h_k - h_{k-1}\right)\{\varepsilon^\circ\} + \frac{1}{2}\left(h_k^2 - h_{k-1}^2\right)\{\kappa\}\right\}$$

$$[M] = Q_{ij}\left\{\left(h_k^2 - h_{k-1}^2\right)\{\varepsilon^\circ\} + \frac{1}{3}\left(h_k^3 - h_{k-1}^3\right)\{\kappa\}\right\} \tag{21}$$

Comparing equations 20 and 21, W' can be obtained as follows.

$$W' = \frac{L}{2}\left(\{\varepsilon^\circ\}^T [N] + \{\kappa\}^T [M]\right) \tag{22}$$

Now the strain energy for the curved element can be obtained by integrating W' within limits θ_1 to θ_2.

$$U_b = \int_{\theta_1}^{\theta_2} \left\{\frac{L}{2}\{\varepsilon^\circ\}^T [N] + \frac{L}{2}\{\kappa\}^T [M]\right\} R\,d\theta \tag{23}$$

From equation 12

$$\begin{Bmatrix} \varepsilon^\circ \\ \kappa \end{Bmatrix} = \begin{bmatrix} A' & B' \\ C' & D' \end{bmatrix} \begin{Bmatrix} N \\ M \end{Bmatrix}$$

$$\begin{Bmatrix} \varepsilon^{\circ} \\ \kappa \end{Bmatrix}^T = \begin{Bmatrix} N \\ M \end{Bmatrix}^T \begin{bmatrix} A' & B' \\ C' & D' \end{bmatrix}^T$$

$$\begin{Bmatrix} \varepsilon^{\circ} \\ \kappa \end{Bmatrix}^T \begin{Bmatrix} N \\ M \end{Bmatrix} = \begin{Bmatrix} N \\ M \end{Bmatrix}^T \begin{bmatrix} A' & B' \\ C' & D' \end{bmatrix}^T \begin{Bmatrix} N \\ M \end{Bmatrix} \quad (24)$$

By suitably re-arranging the terms, it can be obtained in the following form

$$\{\varepsilon^{\circ}\}^T [N] + \{\kappa\}^T [M] = \begin{Bmatrix} N \\ M \end{Bmatrix}^T \begin{bmatrix} A' & B' \\ C' & D' \end{bmatrix}^T \begin{Bmatrix} N \\ M \end{Bmatrix} \quad (25)$$

From the eequations. 23 and 25

$$U_b = \frac{L}{2} \int_{\theta_1}^{\theta_2} \begin{Bmatrix} N \\ M \end{Bmatrix}^T \begin{bmatrix} A' & B' \\ C' & D' \end{bmatrix}^T \begin{Bmatrix} N \\ M \end{Bmatrix} R \, d\theta \quad (26)$$

where

$$R = \frac{a \times b}{\sqrt{\left(a^2 \sin^2\theta + b^2 \cos^2\theta\right)}} \quad (27)$$

'R'-radius of one quadrant of ellipse at any 'θ' between 0 and 90°, which is given by the above equation 27.

Stiffness of the Spring Element

As already stated, because of bi-axial symmetry of the spring element, only one quadrant need to be considered as shown in Fig. 2 To avoid bending-extension coupling

$[A']$= $[A]^{-1}$

$[B']$= 0 since [B*]= 0

$[C']$= 0 since [C*]= 0

$[D']$= $[D]^{-1}$

The equation 26 becomes

$$U_b = \frac{L}{2} \int_{\theta_1}^{\theta_2} \begin{Bmatrix} N \\ M \end{Bmatrix}^T \begin{bmatrix} A' & 0 \\ 0 & D' \end{bmatrix} \begin{Bmatrix} N \\ M \end{Bmatrix} R \, d\theta \quad (28)$$

Referring to the Fig. 3 the above equation can be written as

$$U_b = \frac{L}{2} \times \int_{\theta_1}^{\theta_2} \begin{Bmatrix} N_\theta \\ N_x \\ N_{x\theta} \\ M_\theta \\ M_x \\ M_{x\theta} \end{Bmatrix}^T \begin{bmatrix} \begin{bmatrix} A_{11} & A_{12} & A_{16} \\ A_{21} & A_{22} & A_{26} \\ A_{16} & A_{26} & A_{66} \end{bmatrix}^{-1} & \\ & \begin{bmatrix} D_{11} & D_{12} & D_{16} \\ D_{21} & D_{22} & D_{26} \\ D_{16} & D_{26} & D_{66} \end{bmatrix}^{-1} \end{bmatrix} \begin{Bmatrix} N_\theta \\ N_x \\ N_{x\theta} \\ M_\theta \\ M_x \\ M_{x\theta} \end{Bmatrix} \times R \, d\theta \quad (29)$$

stiffness matrix, the spring element was considered to be made up of mid-plane symmetric laminate.

It is known that, for a symmetric laminate [B] = 0.

Referring to eqns. 9 and 5a

All the stress resultants become zero due to symmetry. Similarly, the moment resultant M_x and $M_{x\theta}$also become zero. The spring is assumed to be made out of specially orthotropic laminate.

$$U_b = \frac{L}{2}\int_0^{\frac{\pi}{2}} M_\theta^2 \; D_{11}^{-1} \; R \; d\theta$$

. M_θ = M/L

$$= \frac{L}{2}\int_0^{\frac{\pi}{2}} \left(\frac{M}{L}\right)^2 D_{11}^{-1} \; R \; d\theta$$

$$U_b = \frac{1}{2L}\int_0^{\frac{\pi}{2}} M^2 \left(\frac{D_{22}\; D_{66} - \; D_{26}^2}{|D|}\right) R \; d\theta \qquad (30)$$

Referring to Fig. 2, the moment M at any section of the spring can be written as

$$M = M_b \; - \; \frac{P}{2} \; (\; a - R \; cos\theta) - H_b R \; sin\theta \qquad (31)$$

where, H_b is fictious and equal to zero.

From the previous derivations, we know that the bending strain energy is given by

$$U_b = \frac{1}{2L} \times D_{11}^{-1} \times \int_0^{\pi/2} M^2 ds$$

$$ds = R \, d\theta$$

$$U_b = \frac{1}{2L} \times D_{11}^{-1} \times \int_0^{\pi/2} \left(M_b - (\frac{P}{2}(a - R \; cos\theta))\right)^2 R \, d\theta \qquad (32)$$

Since the variation of slope (rotation) is zero at 'B. '

$$\frac{\partial U_b}{\partial M_b} = 0$$

$$\frac{\partial U_b}{\partial M_b} = \frac{1}{L} \times D_{11}^{-1} \times \int_0^{\pi/2} \left(M_b - (\frac{P}{2}(a - R \times cos\theta))\right) \times 1 \times R \, d\theta = 0 \qquad (33)$$

The above equation can be written as

$$\int_0^{\pi/2} M_b \; R \, d\theta - \int_0^{\pi/2} \frac{P}{2} \times a \, R \, d\theta + \int_0^{\pi/2} \frac{P}{2} \times R^2 \, cos\theta \; d\theta = 0 \qquad (34)$$

The statically indeterminate bending moment 'M_b'is given as follows:

Due to the above considerations the expression (29) for 'U_b' reduces to the following form.

$$M_b = \frac{P}{2} \times \left[a - \left(\frac{\int_0^{\pi/2} R^2 \times \cos\theta \; d\theta}{\int_0^{\pi/2} R \; d\theta} \right) \right] \quad (35)$$

Calculation of Spring Deflection (δ)

The deflection at the required point (at 'A'- minor axis end) can be obtained using the Castigliano's first theorem, which states that the 'Partial derivative of the strain energy (U_b) with respect to the applied load gives the vertical deflection in the direction of application of the force' i.e. $\frac{\partial U_b}{\partial P} = \delta$.

The equation (27) for 'R' and the expression (35) for 'M_b' can be substituted in expression for U_b(equation 32). The equation for U_b can be partially differentiated with respect to the applied load (P/2) to get the deflection (□□ at the required point. The stiffness (k) of the composite elliptic spring element can be calculated as follows:

k= P/(2□□

□□□□

All the above evaluation of expressions were performed using a computer programme

Stress-Strain Calculations for Composite Elliptic Spring Elements

Strain calculations

$$\{\varepsilon\} = \{\varepsilon^o\} + z\{\kappa\} \quad (37)$$

$$\begin{Bmatrix} \varepsilon_\theta \\ \varepsilon_x \\ \gamma_{x\theta} \end{Bmatrix} = \begin{Bmatrix} \varepsilon_\theta^o \\ \varepsilon_x^o \\ \gamma_{x\theta}^o \end{Bmatrix} + z \begin{Bmatrix} \kappa_\theta \\ \kappa_x \\ \kappa_{x\theta} \end{Bmatrix} \quad (38)$$

It is well known that

$$\begin{Bmatrix} M_\theta \\ M_x \\ M_{x\theta} \end{Bmatrix} = \begin{bmatrix} D_{11} & D_{12} & 0 \\ D_{12} & D_{22} & 0 \\ 0 & 0 & D_{66} \end{bmatrix} \begin{Bmatrix} \kappa_\theta \\ \kappa_x \\ \kappa_{x\theta} \end{Bmatrix} \quad (39)$$

The mid-plane strains $\{\varepsilon^o\}$ were assumed to be zero.

$$\begin{Bmatrix} \varepsilon_\theta \\ \varepsilon_x \\ \varepsilon_{x\theta} \end{Bmatrix} = 0 + z \times \left(\frac{12}{h^3} \begin{bmatrix} Q_{11} & Q_{12} & 0 \\ Q_{12} & Q_{22} & 0 \\ 0 & 0 & Q_{66} \end{bmatrix}^{-1} \begin{Bmatrix} M_\theta \\ M_x \\ M_{x\theta} \end{Bmatrix} \right) \quad (40)$$

Since M_x and $M_{x\theta}$ are zero, the above equation becomes

$$\begin{Bmatrix} \varepsilon_\theta \\ \varepsilon_x \\ \varepsilon_{x\theta} \end{Bmatrix} = z \times \left(\frac{12}{h^3} \begin{bmatrix} \frac{1}{E_{11}} & \frac{-\gamma_{12}}{E_{11}} & 0 \\ \frac{-\gamma_{12}}{E_{11}} & \frac{1}{E_{22}} & 0 \\ 0 & 0 & G_{12} \end{bmatrix}^{-1} \begin{Bmatrix} M_\theta \\ 0 \\ 0 \end{Bmatrix} \right) \quad (41)$$

$$\begin{Bmatrix} \varepsilon_\theta \\ \varepsilon_x \\ \varepsilon_{x\theta} \end{Bmatrix} = z \times \left(\frac{12}{h^3} \begin{bmatrix} \frac{M_\theta}{E_{11}} \\ \frac{-\gamma_{12} M_\theta}{E_{11}} \\ 0 \end{bmatrix} \right) \quad (42)$$

$$M_\theta = \frac{1}{L} \times \left(M_b - \frac{P}{2}\left(a - R \times \cos\theta\right)\right) \quad (43)$$

The above expression for 'M_θ'can be substituted in the eqn. 2.42 and the strains can be evaluated.

Stress calculations

It is well known that

$$\begin{Bmatrix} \sigma_\theta \\ \sigma_x \\ \sigma_{x\theta} \end{Bmatrix} = \begin{bmatrix} Q_{11} & Q_{12} & 0 \\ Q_{12} & Q_{22} & 0 \\ 0 & 0 & Q_{66} \end{bmatrix} \begin{Bmatrix} \varepsilon_\theta \\ \varepsilon_x \\ \varepsilon_{x\theta} \end{Bmatrix} \quad (44)$$

Substituting equation 42 in equation 44

$$\sigma_\theta = Q_{11} \frac{12}{h^3} z \frac{M_\theta}{E_{11}} - \left(Q_{12} \frac{12}{h^3} z \frac{\gamma_{12} M_\theta}{E_{11}} \right) \quad (45)$$

$$\sigma_x = Q_{12} \frac{12}{h^3} z \frac{M_\theta}{E_{11}} - \left(Q_{22} \frac{12}{h^3} z \frac{\gamma_{12} M_\theta}{E_{11}} \right)$$

$$= \left(\gamma_{21} \frac{E_{11}}{1-\gamma_{12}\gamma_{21}} \times z \frac{12}{h^3} \times \frac{M_\theta}{E_{11}} \right) - \left(\frac{E_{22}}{1-\gamma_{12}\gamma_{21}} \times \frac{12}{h^3} \times z \frac{\gamma_{21} M_\theta}{E_{22}} \right) \quad (46)$$

$$= 0$$

So the stresses in the 'x' direction becomes zero. The inplane shear stresses also become zero since it was assumed that the spring element was made up of specially orthotropic laminate.

RESULTS AND DISCUSSION

The results of the theoretical studies have been presented and discussed in this section. To start with the theoretical formulation is validated by comparing the results of So et al

The following Table 1 gives the comparison between stiffness values for circular spring elements predicted by So *et al* and the stiffness values predicted through present formulation. The results of present formulation agree well with the results of So et al. predicted for circular spring. The stiffness values of circular spring elements were evaluated through the present formulation by keeping the a/b ratio as 1.0

Comparison of Spring Stiffness (N/mm) values of circular spring element			
Thickness in (mm)	Volume fraction of Fibers (%) (V_f)	Obtained from reference 1 (*So et al)*	Present formulation
2.49	29.17	27.28	28.8
2.3	34.91	280.96	281.7
7.59	30.84	704.93	706.2

Table 1 Comparison between available and predicted results for circular spring elements

Table 1 Comparison between available and predicted results for circular spring elements. Composite elliptic spring elements of Unidirectional Roving laminate configuration having a/b ratio as 1.5 were fabricated by filament winding technique. The following Fig. 4 shows the split mandrel used for the fabrication of the elliptic spring elements is given in the following.

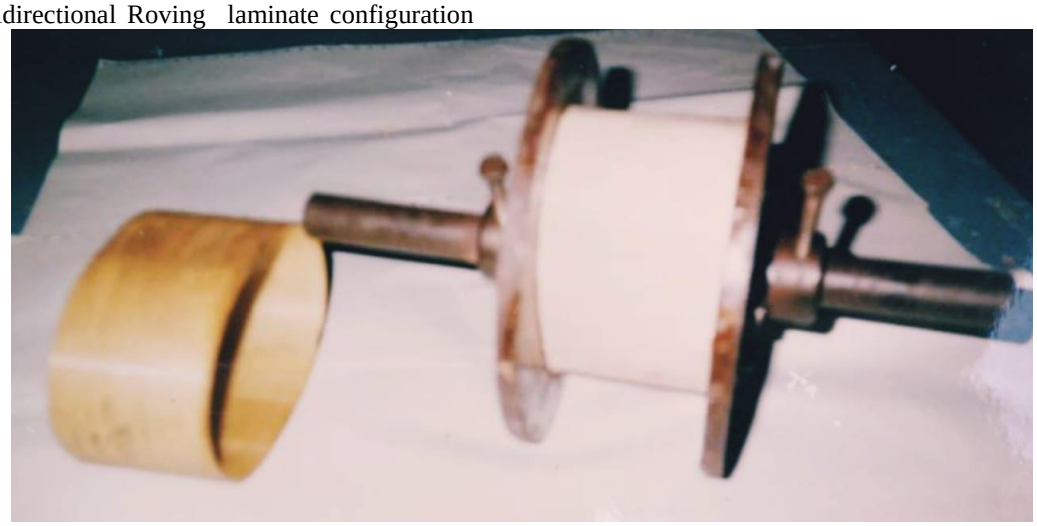

Fig 4 Mandrel used for the fabrication of spring element and sample fabricated spring element

These spring elements were subjected to static stiffness tests and the load-displacement curves were obtained. The tensile modulus of the laminate having 0.45 V_f has been experimentally measured as 29.3 GPa.

From Table 2, it can be observed that the theoretical and experimental stiffness values agree well with each other. However, it can be seen that as the thickness of the spring element increases, the difference (%) between the experimental and the theoretical stiffness values also increases. This is due to the fact that, transverse shear effects increase with the increase in thickness. However the desired spring element stiffness value is around 100N/mm only. In this range the difference is around 5% which quite acceptable for orthotropic materials

Table 2 Comparison of theoretical and experimental stiffness values of elliptic spring elements (UDR spring element, a/b = 1.5 and L=7.5 cm)

Sl.No	Thickness (mm)	Stiffness (N/mm)		Difference (%)
		Theoretical	Experimental	
1	3.0	79.9	76.0	4.87
2	3.5	124.3	117.0	5.8
3	4.0	181.0	168.0	7.1
4	4.5	253.7	235.0	7.37

Prediction of spring performance using the analytical models

The variation of the stiffness of spring element with the increase in thickness is presented in Fig. 5 The stiffness increases as the thickness increases. The increase in stiffness with thickness was found to be non-linear (cubic function). The results also illustrate the influence of a/b ratio on the stiffness of the spring elements. The circular spring element (a/b =1.0) has the highest stiffness. As the a/b ratio increases, the stiffness of the spring element reduces.

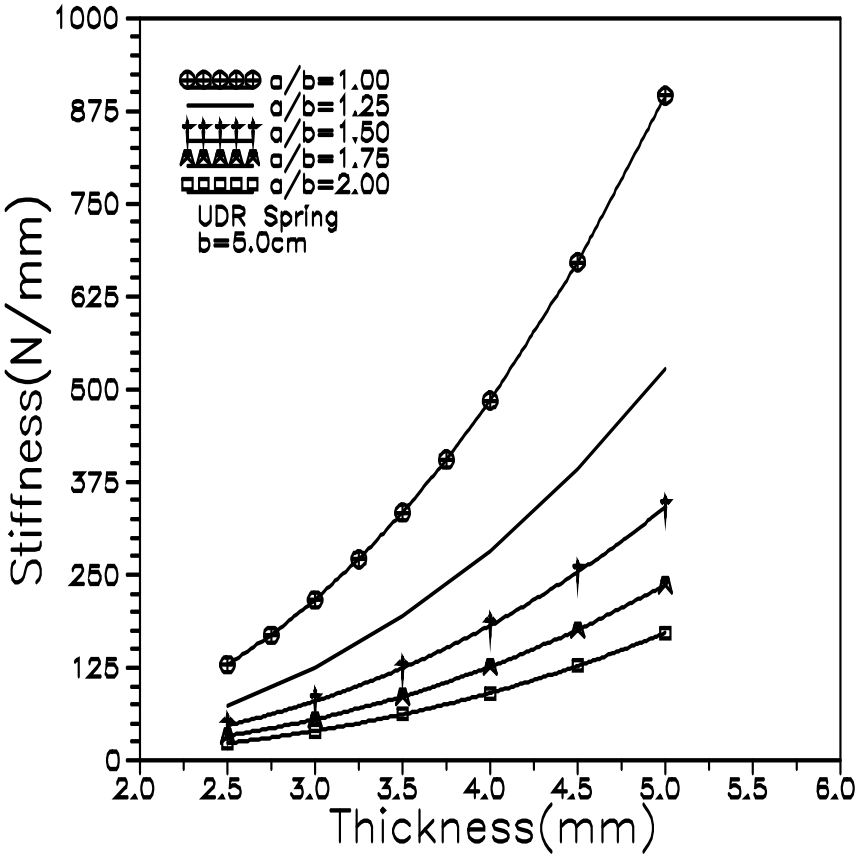

Fig. 5 Variation of stiffness with thickness of the spring element

It can be observed from Fig. 5 that for an increase in a/b ratio from 1.0 to 1.5, the stiffness reduces by a factor of 2.65. Similarly when the a/b ratio increases from 1.5 to 2.0, the stiffness reduces by a factor of 2.0. It can be observed that for a given spring element stiffness any increase in a/b ratio requires an increase in thickness. In the present study, the value of 'b' (semi-minor axis) has been kept constant as 5.0 cm. This selection was based on the standard front suspension spring height. The $V_f$used is 0.45 and spring width is 7.5 cm.

The variation of spring stiffness with a/b ratio for different types of laminate configurations is presented in Fig. 6. The different laminate configurations used in the study are listed in the Table 3. From Fig. 6, it can be observed that the laminate type-4 spring elements give the highest stiffness which is followed by laminate types-1, 3 and 2 respectively. The spring element of laminate type-1 configuration has a stiffness of about 150 N/mm for an a/b ratio of 1.5. The Fig. 5 gives an overall idea about the influence of laminate structure on the stiffness of spring elements. The stiffness characteristics are very much dependent upon the thickness, fibre orientation, V_f of each lamina and geometric position of the different lamina in the laminate.

Table 3 Details of different laminates

Laminate code	Configuration	Thickness (mm)
Laminate -1	(WRM/UDR/WRM/UDR/WRM/UDR/WRM)	4.7
Laminate -2	(UDR/WRM/UDR/WRM/UDR)	3.1
Laminate -3	$(UDR/WRM/UDR)_s$	3.6
Laminate -4	$(WRM/UDR/WRM/UDR)_s$	5.2

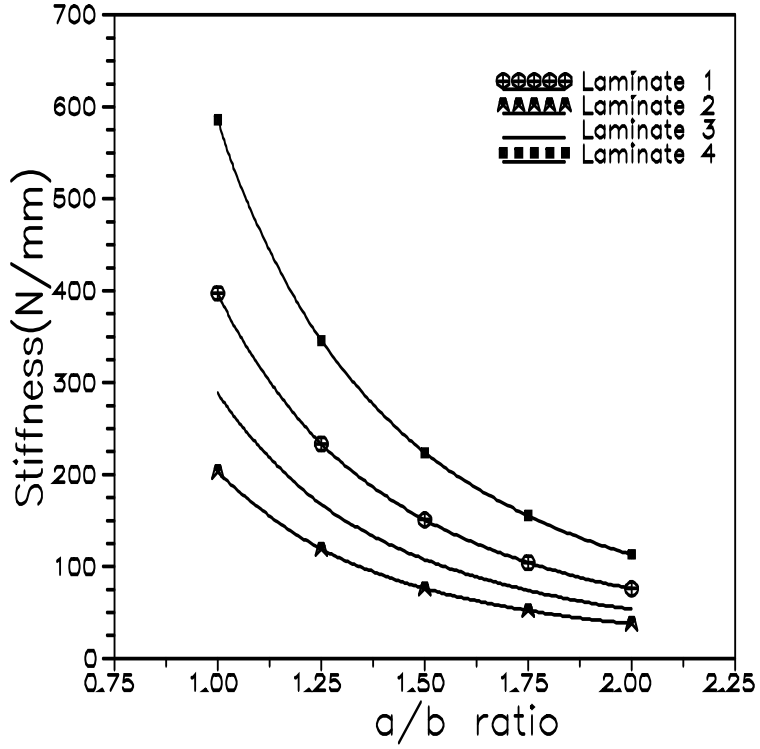

Fig. 6 Variation of spring element stiffness with type of the laminate

The influence of V_f on the stiffness of different types of composite elliptic spring elements is shown in Fig. 7. The $V_f$is an important design factor as far as the energy dissipation properties of the spring element is concerned. Higher V_f suppresses the inherent damping capacity of the polymer matrix, while lower $V_f$will reduce the strength and stiffness of the laminate. Hence an optimum V_f should be selected for the desired damping and mechanical properties.

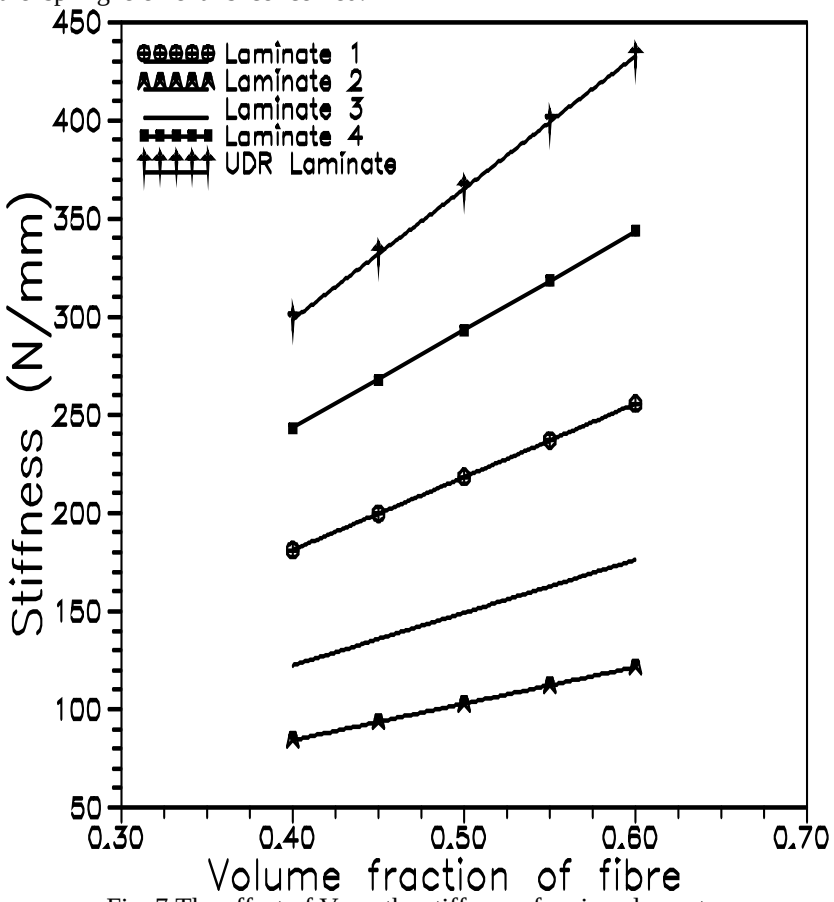

Fig. 7 The effect of V_f on the stiffness of spring elements.

The stiffness increases linearly with V_f. It is observed that an increase in V_f from 0.4 to 0.6 results in about 43% increase in stiffness for all spring elements irrespective of laminate configuration. The results shown in Fig. 7 were obtained for an a/b ratio of 1.5 and the thickness of the UDR spring element as 4.5 mm. Other parameters were kept identical.

The variation of spring element stiffness with its width is shown in Fig. 8. One way of increasing the spring stiffness (according to the vehicle requirements) is to increase the thickness of the spring element. However, this could lead to undesirable transverse shear effects, which could affect the performance of the spring. The stiffness increases linearly with the width of the spring element. This result assumes greater importance, since the spring stiffness can be increased considerably without increasing the thickness or V_f.

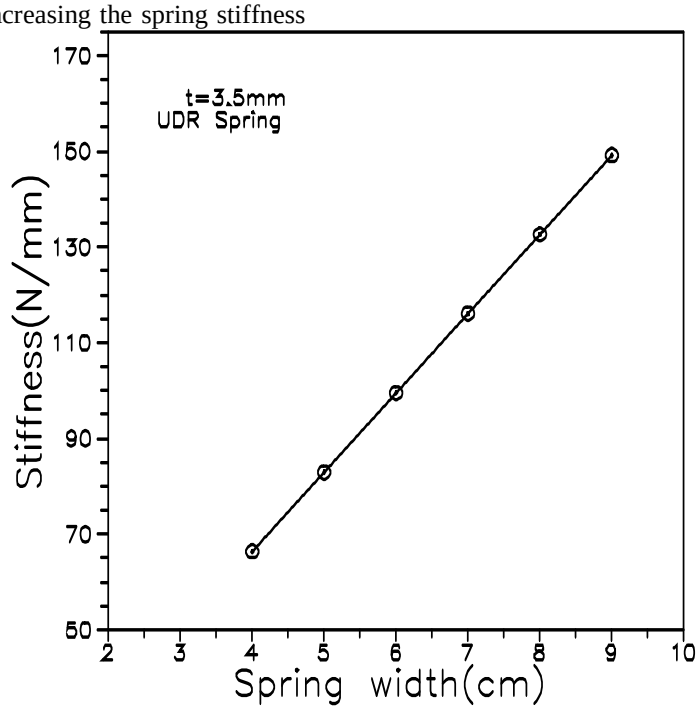

Fig. 8 Change in the spring element stiffness with the width

If the space is not a constraint for fixing the suspension system, the best way to enhance the stiffness of the spring element is to increase its width. By increasing the width, load bearing area of the spring element also increases. This will reduce the magnitude of the stress acting on the laminate, leading to an increase in the fatigue life of the spring element. The results of the Fig. 8 were obtained for a V_f of 0.45 and an a/b ratio of 1.5.

Variation of bending moment along the one quadrant (0-90°) of spring elements having different a/b ratios is presented in the Fig. 9. It can be observed that the bending moment increases as the a/b ratio increases. For the same load, higher bending moment results in higher bending strain energy.

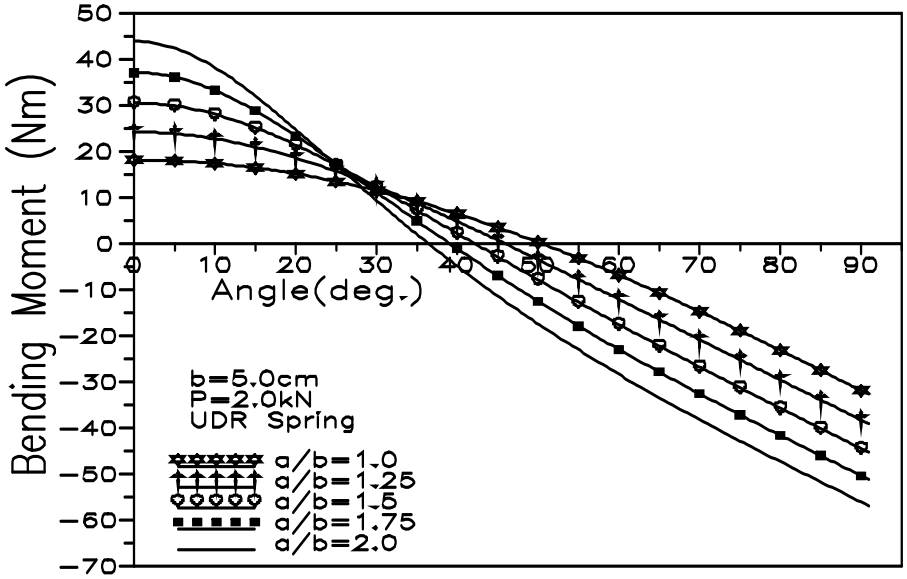

Fig. 9 Variation of bending moment along the one quadrant of different spring elements

From these curves (Fig.9), the point of contraflexure (where the bending moment becomes zero) can be clearly obtained. The point of contraflexure was found to be of great importance in the development of composite elliptic springs. At these locations it is preferable to fix high damping elastomers (or rubber inserts), so that the damping capacity of the composite spring suspension system can be increased. The point of contraflexure tends to be closer to the major axis as the a/b ratio increases. The results of Fig. 9 were obtained for a V_f of 0.5 keeping other parameters to be the same.

The variation of bending stress (for one quadrant) with the spring element width is given in Fig. 10. It can be observed that the stresses decrease as the spring width increases. These results were obtained for an a/b ratio of 1.5 keeping other parameters to be the same.

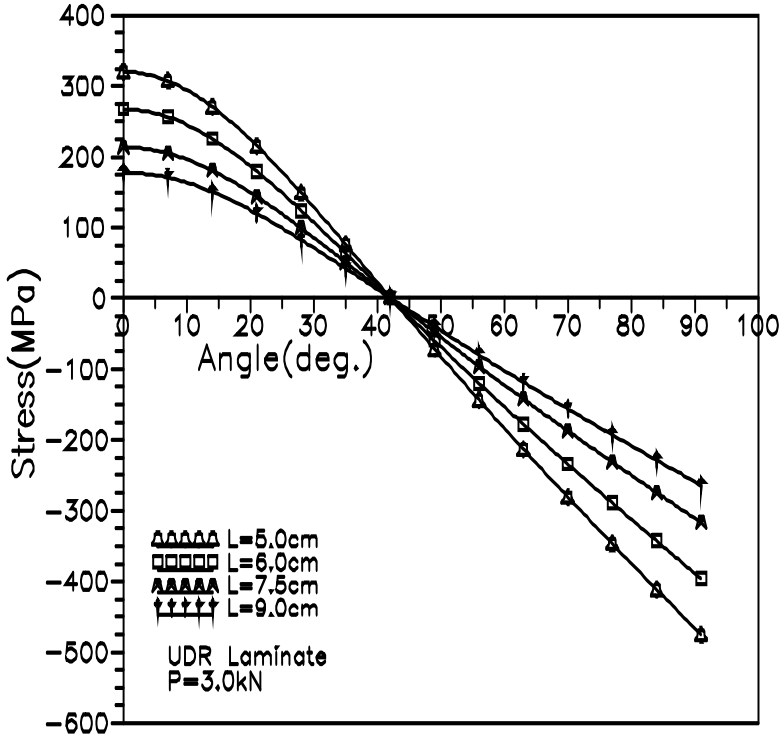

Fig. 10 Influence of width of the spring elements on the laminate stress.

The effect of variation of spring element thickness on the laminate stresses is shown in Fig.11 As the thickness increases, the load bearing area of the spring element also increases leading to the reduction in laminate stress. A V_f of 0.5, a/b ratio of 1.5 and a width of 7.5 cm were used in obtaining the results of Fig. 11.

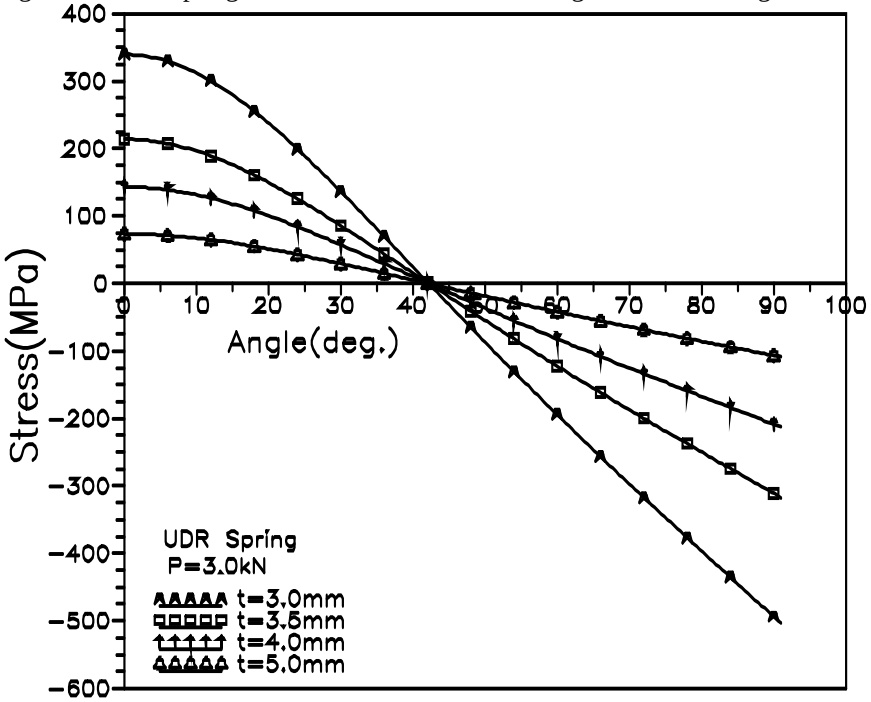

Fig 11 Stress variation along one quadrant of the UDR spring element for different

laminate thickness

The strain variation along one quadrant of the spring element is given in Fig. 12. It can be observed that as the a/b ratio increases the laminate strain also correspondingly increases.

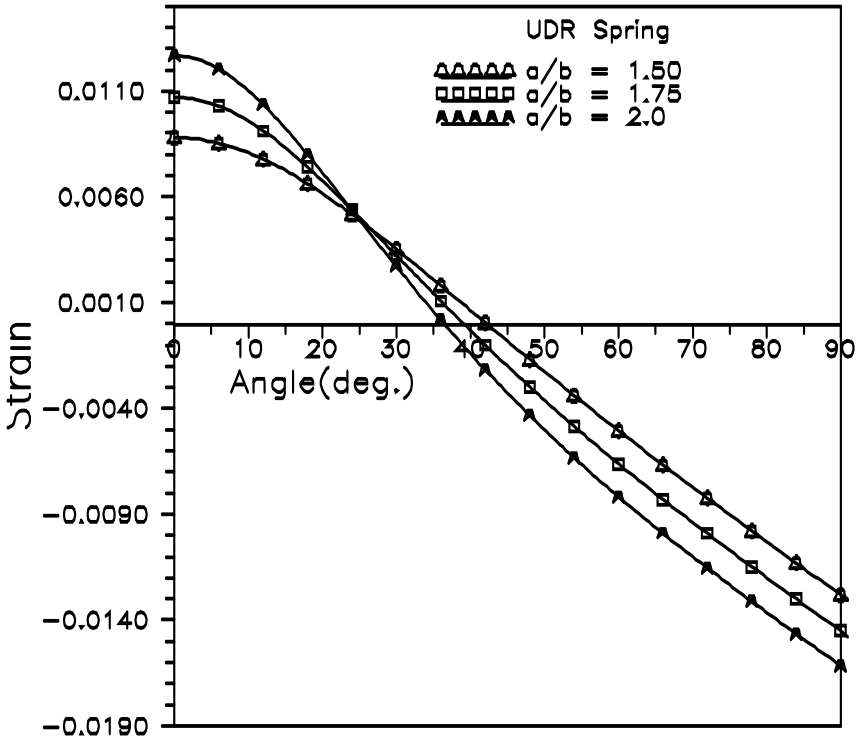

Fig. 12 Strain distribution along the one quadrant of the spring element for different a/b ratios.

Typical stress variation across the thickness of laminate type-1 spring element has been shown in Fig13. Because of symmetry, the stress variation through half of thickness alone has been presented. In the present analysis, the WRM lamina has been considered as individual 0° and 90° plies. The topmost ply corresponds to 0° lamina of woven roving mat , which takes proportionately higher stresses. The topmost lamina is immediately followed by the 90° lamina of WRM. The 90° lamina takes proportionately less stress.

It can be observed from Fig. 13 that the stress distribution through the laminate thickness is not linear. The stresses are discontinuous at the interface of two laminae and the stress gradient in two adjoining laminae is also different. The stress distribution within each ply varies linearly. The UDR lamina takes the maximum stresses owing to its orientation of fibres in the direction of the applied stress.

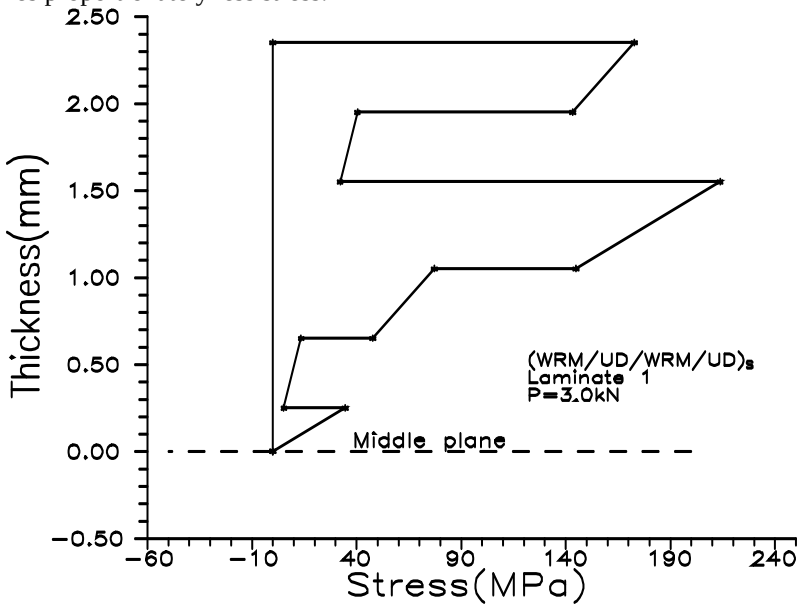

Fig. 13 Stress variation across the thickness of the laminate type-1 at major axis end.

Referring to the Fig. 13, the type of stress variation across the thickness of the laminate could be attributed to the following facts.

(i) Orientation of fibre.

(ii) V_f of each lamina.

(iii) Geometric position of the lamina in the laminate.

The typical strain variation across the thickness of the laminate type-1 spring element has been given in Fig. 14.

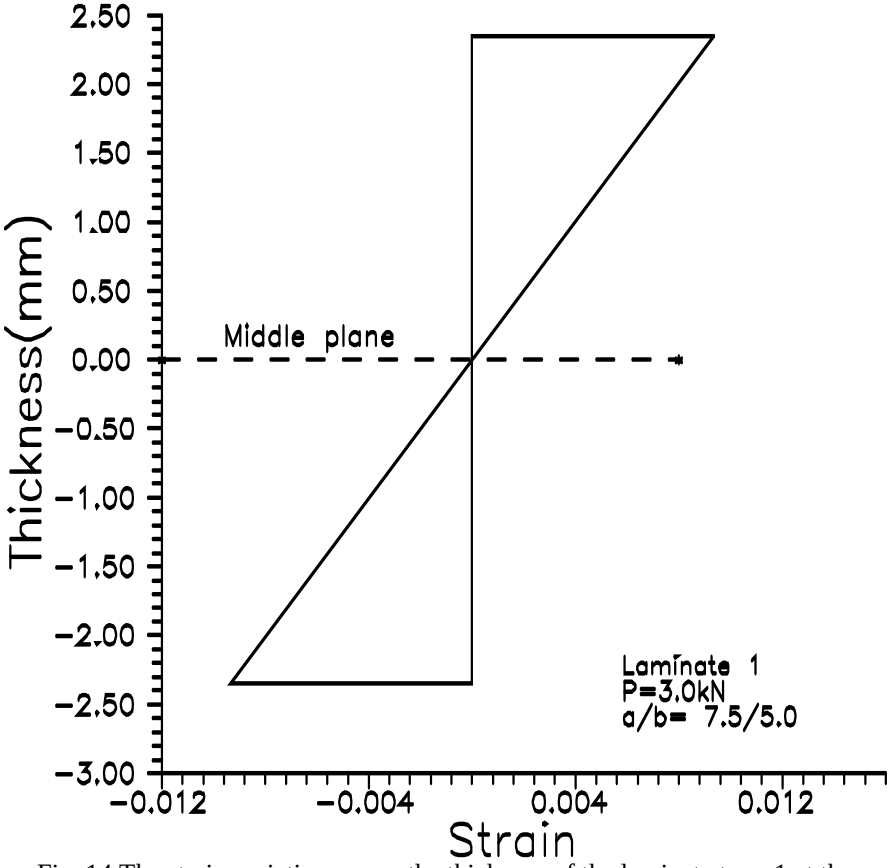

Fig. 14 The strain variation across the thickness of the laminate type-1 at the major axis end.

It can be observed that unlike the stress variation, the strain variation was found to be continuous and linear throughout the laminate thickness. The difference in the moduli of each lamina can account for the variation in the stress amplitude (Fig. 13) despite the linear variation of strain.

Conclusions

The stiffness values of the spring elements obtained by theoretical analysis and experimental studies agree well. The validity of the formulation was verified with already available results in the literature for circular composite spring elements. They agree well. From the present study it can be understood that the spring element stiffness is very much influenced by the following major spring parameters:

(a) Laminate thickness.

(b) a/b ratio.

(c) Width of the spring.

(d) Fibre volume fraction.

(e) Laminate configuration.

The spring element stiffness increases in a non-linear (cubical) fashion with the increase in the thickness. The spring element stiffness reduces with the increase in the a/b ratio. When the a/b ratio was increased from 1.0 to 1.5, the stiffness reduces by a factor of 2.65 irrespective of laminate configurations. Similarly the stiffness reduces by a factor of 2.0 when the a/b ratio was increased from 1.5 to 2.0. The stiffness increases linearly with the increase in width of spring element.

The stiffness varies linearly with the variation in the increase in V_f . The increase in V_f from 0.4 to 0.6 results in an increase in the stiffness by about 43%. The bending moment acting along the one quadrant increases with the increase in a/b ratio. From the bending moment results, the point of contraflexure can be identified for each a/b ratio. The stress which act along the one-quadrant of the spring element decreases as the width of the spring element increases. Similarly the laminate stress decreases as the thickness of the spring element increases. The spring laminate is subjected to maximum stress at the ends of their major and minor axis.

This stress distribution across the thickness of the laminate is mainly dependent upon the following variables:

(i) Direction of fibre orientation in the lamina.

(iii) Geometric position of the individual ply within the laminate.

(iv) $V_f$of each lamina.

General Comments:

1. Equation part need to be reduced sir,
2. Over all paper is excellent sir , we should remove the terminology or oror in-between the equations.

References:

1. **So, C.K., P.C.Tse, T.C.Lai,** and**M.Young**(1991**)** Static mechamicalbehaviour of composite cylindrical springs, *Compos Sci. and Technol.*, **40**, 251-263.

2. E. Mahdi ,O.M.S. Alkoles , A.M.S. Hamouda , B.B. Sahari , R. Yonus , G. Goudah 'Light composite elliptic springs for vehicle suspension' Composite Structures 75 (2006) 24–28

3. Abdul Rahim Abu Talib , Aidy Ali b, G. Goudah, Nur Azida Che Lah and A.F. Golestaneh 'Developing a composite based elliptic spring for automotive applications' Materials and Design 31 (2010) 475–484

4. Amol Bhanage and K. Padmanabhan 'Design for fatigue and simulation of glass fibre/epoxy composite automobile leaf spring' ARPN Journal of Engineering and Applied Sciences, VOL. 9, NO. 3, MARCH 2014

5**.** Shivaji M. Mane and S B. Bhosale 'Design and Analysis of Elliptical Leaf Spring for Light Agricultural Machines with CFRP Material' International Journal of Engineering Research & Technology Vol. 5 Issue 06, June-2016

6. W. Papacz, E. Tertel and P. Kuryło 'Performance comparison of conventional and composite leaf spring' Journal Of Measurements In Engineering. March 2014, Volume 2, Issue 1 pp: 24-28

7.P. K. Mallick 'Static Mechanical Performance of Composite Elliptic Springs' Transactions of the ASME 22/Vol. 109, JANUARY 1987

8. P.C. Tse , K.J. Lau , W.H. Wong ,and S.R. Reid 'Spring stiffnesses of composite circular springs with extended flat contact surfaces under unidirectional line-loading and surface-loading configurations' -Composite Structures 55 (2002) 367–386

9. P.C. Tse, S.R. Reid , K.J. Lau , W.H. Wong 'Large deflections of composite circular springs with extended flat contact surfaces' Composite Structures 63 (2004) 253–260

10) P. C. Tse, S R Reid and S P Ng 'Spring constants of filament-wound composite circular rings'Journal of Mechanical Engineering Science2001 pp: 211-215

11)Nahit Oztoprak, Mehmet Deniz Gunes, MetinTanoglu, EnginAktas, CilerSenocak and GedizKulac 'Developing polymer composite-based leaf spring systems for automotive industry' Science and Engineering of Composites 2018; 25(6): 1167–1176

12) Zheng Yinhuan, Xue Ka and Huang Zhigao ' Finite Element Analysis of Composite Leaf Spring' The 6th International Conference on Computer Science & Education (ICCSE 2011) August 3-5, 2011. SuperStar Virgo, Singapore

13) Anil Antony Sequeira, Ram Kishan Singh and Ganesh K. Shetti '
Comparative Analysis of Helical Steel Springs with Composite Springs Using Finite Element Method' Journal of Mechanical Engineering and Automation 2016, 6(5A): 63-70

14) Mehdi Bakhshesh and Majid Bakhshesh **'**Optimization of Steel Helical Spring by Composite Spring' International Journal Of Multidisciplinary Sciences And Engineering, Vol. 3, No. 6, June 2012

GLOSSARY

[A], [B], [D] = Constitutive matrices of the laminate
E_{11}, E_{22} = Young's Modulus in the principal material directions
M, M_B = Bending moment
P = Uniaxial load
G_{12} = Shear modulus with reference to principal axes
h = Thickness of the shell
L = Width of the shell
[M] =Moment resultants
[N] =Stress resultants
[Q] = Lamina stiffness matrix referring to principal axes
R =Radius of the midplane of the shell
[S] = Lamina compliance matrix referring to principal axes
U_b =Strain energy
δ =Vertical displacement of the spring
V =Volume of the shell
W = Strain energy density function
W' = Strain energy density function for the crosssectional area
z =Distance from the mid-surface
ε = Strain
[$\varepsilon°$] = Mid-plane strain
[κ] = Mid-surface curvature
ν_{12} =Major Poisson ratio
σ = Stress
a = Semi-major axis
b = Semi-minor axis
θ = Angle from semi-major axis
R = Radius of elliptic spring element at any given angle 'θ'

c